Interference Avoidance through Pilot-Based Spectrum Sensing Algorithm in Overlaid Femtocell Networks

Padmapriya Sambanthan and Tamilarasi Muthu

Co-channel interference between macro–femtocell networks is an unresolved problem, due to the frequency reuse phenomenon. To mitigate such interference, a secondary femtocell must acquire channel-state knowledge about a co-channel macrocell user and accordingly condition the maximum transmit power of femtocell user. This paper proposes a pilot-based spectrum sensing (PSS) algorithm for overlaid femtocell networks to sense the presence of a macrocell user over a channel of interest. The PSS algorithm senses the pilot tones in the received signal through the power level and the correlation metric comparisons between the received signal and the local reference pilots. On ensuring the existence of a co-channel macrocell user, the maximum transmit power of the corresponding femtocell user is optimized so as to avoid interference. Time and frequency offsets are carefully handled in our proposal. Simulation results show that the PSS algorithm outperforms existing sensing techniques, even at poor received signal quality. It requires less sensing time and provides better detection probability over existing techniques.

Keywords: Macrocell user, femtocell, co-channel interference, spectrum sensing, power optimization, time offset, frequency offset.

Manuscript received Sept.17, 2014; revised July16, 2015; accepted Aug. 25, 2015.

Padmapriya Sambanthan (corresponding author, padmaece.r@pec.edu) and Tamilarasi Muthu (tamilarasim@pec.edu) are with the Department of Electronics and Communication Engineering, Pondicherry Engineering College, Puducherry, India.

I. Introduction

Telecommunication has come a long way from Graham Bell's wired telephone to wireless multimedia services. Cellular networks play a vital role in wireless communication hierarchies, and network operators are driven toward the challenge of guaranteeing ubiquitous voice and data services. The traditional macro base station (MBS) provides limited coverage to indoor and edge subscribers because of inferior received signal quality and penetration losses [1]. Small-cell technology has been born out of the necessity to handle challenges such as the growing traffic burden, increasing spectral demand, and the need for high data rate multimedia services in indoor environments.

A femtocell — a subset of the small-cell family — is a short-range, low-power plug-and-play base station; such a station is capable of bringing a network closer to its users. Furthermore, it extends voice and multimedia services to macrocell users who are in indoor, coverage hole, shadow, and edge regions. The femtocell has carved a niche for itself due to its potential for traditional network compatibility, higher data rate indoor services, coverage extension to macrocell users, and insignificant greenhouse gas emissions.

Network operators prefer to assign the same uplink frequency band to those macrocell users and femtocell users who are geographically far apart. This method of frequency assignment improves the spectral efficiency and network capacity. Nevertheless, the frequency reuse scenario leads to severe co-channel interference and QoS degradation for users of the primary network, so-called macrocell users [2]. Co-

http://dx.doi.org/10.4218/etrij.16.0114.1087

channel interference becomes severe on account of unplanned and exponential femtocell deployment; access mode selection; and proximity of co-channel users and their dominant transmit power. To handle such situations in macro–femtocell networks, a femtocell base station (FBS) must sense a channel, acquire knowledge about the presence of co-channel macrocell users, and accordingly control their maximum transmit power. These objectives can be met through cognitive radio technology, which is designed to assist a femtocell user in dynamically adjusting a radio parameter upon experiencing interference. In addition, flexible radio parameter adjustment enables heterogeneity and interoperability in femtocell networks [3]–[5].

Spectrum sensing techniques, such as energy detection, cyclostationary detection, and waveform-based detection, can serve secondary femtocells to sense a channel. Energy detectors of low complexity do not require knowledge of macrocell user signal characteristics [6]. In the energy detection technique in [6], the energy of a received signal is compared with a threshold value. If the received signal is weaker than the threshold value, then the channel of interest is determined to be idle; and vice versa.

A cyclostationary detection technique [7] senses the periodic nature of a received signal. Intentionally introduced bits or periodically-phase-shifted signals assist this type of cyclostationary-based spectrum sensing technique. In waveform-based spectrum sensing techniques [8], known patterns, such as *preamble* and *midamble*, and regularly inserted pilot symbols in the transmitted signal serve the secondary network user in identifying a channel's status. Many literatures consider a combination of two to three spectrum sensing techniques in an attempt to mitigate each individual technique's own limitations [9]–[12]. However, combining different spectrum sensing techniques can lead to huge system complexity.

Waveform-based or pilot-based spectrum sensing (PSS) techniques can handle co-channel interference efficiently. Lu and others [13] presented a pilot-assisted spectrum sensing algorithm, which considers the difference between first-order and second-order statistical properties of pilots. Nevertheless, this algorithm requires lengthy differential operations to decide the idleness of a channel. A spectrum sensing technique with cooperative game theory has been addressed in [14]; such a technique flexibly adjusts both the access mode and the power to mitigate interference. However, the technique in [14] requires cooperation from neighboring nodes, which affects the convergence of a system.

Wang and others [15] proposed an interference coordination scheme to sense a spectrum and statistically analyze the radio propagation path loss between femtocell users and macrocell users. Yet, this approach is not a straight forward one in terms of interference handling; it fails to make decisions on weak received signals. The proposal in [16] employs orthogonal time-frequency sensing as well as a radio assignment solution for interference management in macro–femtocell networks. Codebook information sensed through an antenna is utilized to handle intra-tier interference. Nonetheless, the approach in [16] calls upon many complex techniques to handle a single issue.

Min and others [17] suggested two models (namely, cognitive-based cooperative relay model and interference model) to avoid interference between macrocell users and femtocell users. In the former model, femtocells restrict their own transmission during a channel occupancy period of a macrocell user so as to attain effective service quality in any successive communication periods. In the latter model, a femtocell user reduces the transmit power when a macrocell user is busy on a channel of interest. The above cognitive-enabled cooperative decisions, however, affect the throughput of femtocells.

To address challenges such as low signal-to-noise ratio (SNR) sensitivity, hardware complexity, synchronization error, and system convergence, we suggest a simple PSS algorithm with power optimization to handle co-channel interference between macro–femtocell networks. The PSS algorithm senses a channel by tracking the pilot tones on the received signal, thereby determining the presence of a macrocell user over the channel of interest.

Our PSS algorithm treats a received signal over two different stages; namely, coarse detection stage and fine detection stage. In the coarse detection stage, the power of the received signal is compared with that of the local reference pilots as well as the noise floor. If the sensed signal indicates the presence of a macrocell user, then the coarse detection stage instantaneously declares the channel state as "busy," thereby ignoring the rest of the algorithm. This leads to a reduced decision time and minimum sensing unit involvement. If the received signal fails to meet the conditions of the coarse detection stage, then a further stage — fine detection stage — is invoked to determine the channel state.

Even in the presence of frequency offset, time offset, and higher noise gain, the PSS algorithm outperforms other traditional approaches in that it has a smaller network-knowledge acquisition time, weaker macrocell user signal detection, instantaneous interference avoidance, minimal false alarm probability, and maximal probability of detection.

The rest of this paper is organized as follows. Section II presents a brief overview of an orthogonal frequency-division multiplexing (OFDM) system and FBS sensing unit. Section III elaborates on our PSS algorithm, while Section IV analyses the simulation results. Section V outlines our

conclusions.

II. System Model

OFDM techniques are widely used in emerging wireless standards to achieve higher data rates. We analyzed our PSS algorithm with respect to the LTE-OFDM standard [18], where macrocell and overlaid femtocells adopt to an LTE radio propagation model as well as the specifications of a particular OFDM technique.

1. OFDM System

A macrocell user's raw data undergoes convolution coding, 16-QAM process, pilot insertion, and serial-to-parallel conversion. An inverse fast Fourier transform block is used to transform 64 parallel data sequences into a time-domain signal, which can be written as

$$x(n) = \sum_{k=0}^{N-1} X(k) e^{\frac{j2\pi kn}{N}}, \quad (1)$$

where $x(n)$ denotes the nth OFDM signal in the time domain, $X(k)$ denotes the frequency-domain signal, and N denotes the total number of subcarriers. Here, $x(n)$ is up-converted to a radio frequency signal and transmitted over a channel possessing Rayleigh properties.

2. Sensing Unit

A secondary femtocell or FBS must sense the channel of interest to make certain of the existence of a macrocell user. However, due to Doppler effects, a macrocell user's signal may spread in subcarrier guard space. As a result, there is the possibility of frequency offset in the sensed signal. Hence, signal spread in the guard band should also be considered at the FBS to acquire complete channel knowledge.

Let B be the channel of interest and G be the guard space between neighboring channels, as depicted in Fig. 1. If $G/2$ is the space on either side of channel B, over which the Doppler spread is expected, then the total band size to be sensed, S, is expressed as

$$S = \left(\frac{G}{2} + B + \frac{G}{2} \right). \quad (2)$$

To tackle frequency offset in the sensed signal, the FBS must sense the total band size of S, which may happen to contain a macrocell user signal with Doppler spread.

A block diagram of the proposed sensing system is illustrated in Fig. 2. The sensed signal from the RF front end undergoes analog-to-digital conversion (ADC), which converts the continuous time-domain signal, $y(t)$, into a discrete time-domain signal, $y(n)$.

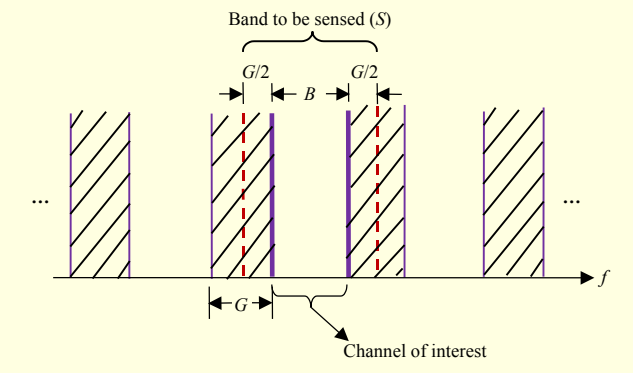

Fig. 1. Illustration of channel of interest and band to be sensed.

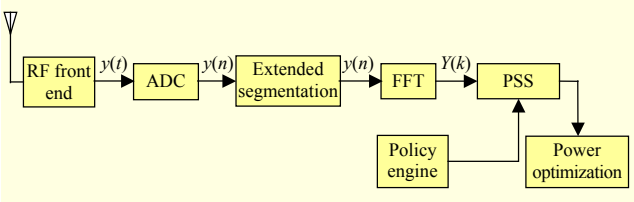

Fig. 2. Block diagram of spectrum sensing unit.

Initially, the existence of a macrocell user in the channel is unknown; hence, it is impossible to predict the exact instant at which the macrocell user begins transmission. Therefore, to meet time synchronization, extended segmentation is introduced to precisely segment the received signal in a synchronized manner. A time offset within a sensing duration causes a phase rotation on the recovered signal in the frequency domain.

A down-converted frequency-domain signal, $Y(k)$, from a fast Fourier transform (FFT) block is given by

$$Y(k) = \frac{1}{\sqrt{N}} \sum_{n=0}^{N-1} y(n) e^{\frac{-j2\pi(k+\Delta k)(n+\Delta n)}{N}} + w(n), \quad (3)$$

where $(k + \Delta k)$ and $(n + \Delta n)$ represent the frequency and time offsets, respectively, in the sensed signal; $w(n)$ is an additive white Gaussian noise with zero mean and unit variance. With the aid of the local reference pilot and FFT processed signal, the PSS algorithm decides the channel state. Under the supervision of a policy engine, only pilot tones are involved as sensing references, which guarantees information security to the co-channel macrocell user.

3. Locally Generated Pilot Tones

The two types of pilot insertion pattern in the OFDM system are regular- or comb-based pilot insertion and scattered pilot insertion [19]. In the comb-based type, the positions of pilot

tones is uniform, whereas in the scattered-based type, the relative positions of the pilot tones varies between successive OFDM symbols. We adopt the comb-based pilot insertion scheme, where the pilots are inserted after 6 or 12 data symbols. We choose to follow pilot insertion after every 12 data symbols, which holds good even for a system that follows pilot insertion after 6 data symbols.

The power of pilot tones will be greater than the power of data symbols. Since both macro- and femtocells follow the LTE signaling standard, femtocells adhere to the pilot insertion pattern of a macrocell network. The FBS is capable of generating local reference pilots from the knowledge of a predefined pilot sequence of a macrocell user's OFDM signal. At transmitter entity, pilot symbols are inserted after every 12 data symbols. Obviously, at the FBS sensing unit, a local pilot sequence is generated in such a way that the successive tones are separated by 12 symbol duration. With reference to local reference pilots, decisions are made by the PSS algorithm resulting in any one of the following hypotheses.

4. Spectrum Sensing Hypotheses

The two well-known important hypotheses of the spectrum sensing algorithm are as follows:

$$\mathcal{H}_0 : Y(k) = w(k), \tag{4}$$

$$\mathcal{H}_1 : Y(k) = x(k) + w(k). \tag{5}$$

The test statistic $\mathcal{H}_0$ denotes the absence of a macrocell user over the channel of interest, and $\mathcal{H}_1$ refers to the presence of a macrocell user over the channel of interest. The performance of the spectrum sensing algorithm is determined by the probability of detection (P_d) and probability of false alarm (P_f), which are formulated as follows:

$$P_d : \left(\mathcal{H}_0 | \mathcal{H}_0\right) \text{ or } \left(\mathcal{H}_1 | \mathcal{H}_1\right), \tag{6}$$

$$P_f : \left(\mathcal{H}_1 | \mathcal{H}_0\right) \text{ or } \left(\mathcal{H}_0 | \mathcal{H}_1\right), \tag{7}$$

where P_d implies the probability of identifying the channel as busy, when the channel is truly busy, and vice versa; P_f is the probability of identifying the channel of interest as busy, when it is truly idle, and vice versa.

5. Signal Sensing Duration

Signal sensing duration plays a vital role in the PSS algorithm. We have chosen the sensing duration in such a way that the acquired channel knowledge is completely sufficient to decide the channel state.

Our PSS algorithm senses the channel of interest for a duration of τ_T, which is given by

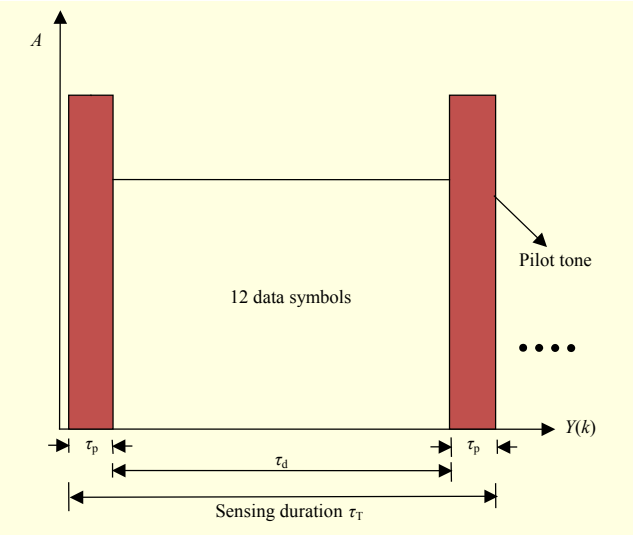

Fig. 3. Representation of macrocell user's pilot tones and sensing duration.

$$\tau_T = \tau_P + \tau_d + \tau_P, \tag{8}$$

where τ_P is the duration of a pilot tone and τ_d is the duration of 12 data symbols (see Fig. 3). Over this duration, the sensing unit senses at most two pilot tones present in the OFDM modulated signal, thereby predicting the existence of a co-channel macrocell user. In addition to the extended segmentation unit, consideration of two pilot durations helps in tracking at least one high-power pilot tone, thereby handling time offset in the sensed signal.

III. Pilot-Based Sensing Algorithm

In a coexisting macro–femtocell network, femtocells are the supplementary service providers and are intended only for use with the residual spectrum. As femtocells operate on a licensed frequency band (one that could be acquired by macrocell users), there exists the threat of co-channel interference. To protect primary macrocell users from interference, secondary femtocells must sense the channel before utilizing it. On sensing the co-existence of macrocell users, the femtocells should condition their maximum transmit power. Our interference avoidance system senses the channel through the proposed PSS algorithm.

Figure 4 illustrates the steps involved in our PSS algorithm. It comprises of two distinct, but inter-dependent stages; namely, a coarse detection stage and a fine detection stage. For every τ_T sensing duration, the test statistic of any one stage determines the channel state. The channel sensing process is considered to be a continuous, back-end process, carried out by

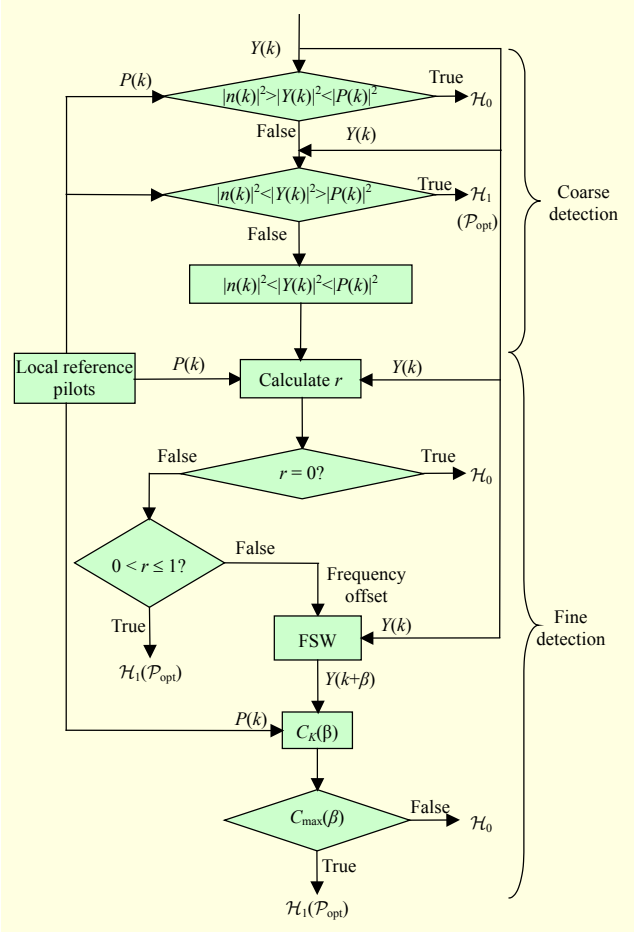

Fig. 4. PSS algorithm.

a "PSS-enabled FBS" throughout its communication period.

1. Coarse Detection Stage

The first stage of our PSS algorithm is the coarse detection stage. It consists of power level comparators, which check the received signal power with the power of locally generated pilot tones and the noise floor.

Let $P(k)$ be a local reference pilot, each such pilot is spaced apart from the next by 12 symbol durations. Let $n(k)$ be the noise floor, which is the sum of all noise sources in the wireless channel. From a link budget analysis of the LTE radio propagation model [18], it is learned that the maximum allowable noise floor for a 10 MHz bandwidth is –116.4 dBm. Hence, the idle channel decision is made with reference to the noise floor value of the LTE standard. The power of the modulated narrowband signal (–12 dBm) will be relatively higher than the power of the channel's noise floor, thereby making a primary user signal immune to any channel impairments.

Let $Y(k)$ be the sensed signal, treated through the RF front end of an FBS. The signal $Y(k)$ undergoes the following possible checks at a power level comparator. Firstly, if the power of the received signal is less than the powers of the noise floor and reference pilot tones, then the channel state is determined as idle. As the pilots are supposed to have higher power, the weak received signal implies the absence of pilot and data signals over the channel of interest. Hence, the test statistic is expressed as follows:

$$\{|n(k)|^2 > |Y(k)|^2 < |P(k)|^2\} : \mathcal{H}_0. \tag{9}$$

On the other hand, if the received signal power is greater than the powers of the noise floor and reference pilot tones, then the presence of high-power pilot tones is ensured and the test statistic then becomes

$$\{|n(k)|^2 < |Y(k)|^2 > |P(k)|^2\} : \mathcal{H}_1. \tag{10}$$

With the hypothesis prediction of $\mathcal{H}_1$, the channel of interest is determined as busy. Hence, the maximum transmit power of a co-channel femtocell user is optimized to protect the on-going transmission of the primary macrocell user from interference. If we denote the maximum transmit power of a interfering femtocell user to be P_{fu}, the received power of a primary macrocell user to be P_{MU}, and the variance of a macrocell user to be δ^2_{MU}, then the optimized power, $\mathcal{P}_{\text{opt}}$, of a co-channel femtocell user is given by

$$\mathcal{P}_{\text{opt}} = \min\left(P_{\text{fu}}, \frac{P_{\text{MU}} + \delta^2_{\text{MU}}}{P_{\text{fu}}}\right). \tag{11}$$

A maximum transmit power optimization allows the survival of both a femtocell user and a macrocell user under the same space, time, and frequency premises. However, if both the test statistics indicated in (9) and (10) fail, then a possible conclusion of the coarse detection stage could be formulated as follows:

$$\{|n(k)|^2 < |Y(k)|^2 < |P(k)|^2\} : \text{uncertain state}. \tag{12}$$

Whenever the condition in (12) prevails in the coarse detection stage of the PSS algorithm, the received signal is found to have a power level lying between that of the noise floor and pilot tone limits. Upon suspecting such uncertainty, the fine detection stage is invoked to clearly identify the channel state.

2. Fine Detection Stage

The fine detection stage calculates the correlation coefficient (r) between $Y(k)$ and $P(k)$, on observing the uncertainty in the received signal. The correlation coefficient measures the linear relationship between two variables and yields a value between +1 and –1 inclusive; that is, $-1 \le r \le 1$. A positive value of r

implies a strong correlation between the two variables, whereas zero and negative values infer null and weak correlations, respectively. The correlation coefficient between the received signal and the local reference pilot is given by

$$r = \frac{\frac{1}{N}\sum_{k=0}^{N-1}[Y(k)\times P(k) - \bar{Y}(k)\times \bar{P}(k)]}{C_{\mathrm{Y}} \times C_{\mathrm{P}}}, \quad (13)$$

where $\bar{Y}(k)$ and $\bar{P}(k)$ are the mean of $Y(k)$ and $P(k)$, respectively, and N is the total number of tones over the sensing duration τ_{T}. The values of $\bar{Y}(k)$ and $\bar{P}(k)$ are obtained through

$$\bar{Y}(k) = \frac{1}{N}\sum_{k=0}^{N-1} Y(k), \quad (14)$$

$$\bar{P}(k) = \frac{1}{N}\sum_{k=0}^{N-1} P(k). \quad (15)$$

In (13), C_{Y} is the covariance of the received signal and C_{P} is the covariance of the local pilot signal. They are given as

$$C_{\mathrm{Y}} = \sqrt{\frac{1}{N}\sum_{k=0}^{N-1}[Y(k)^2 - \bar{Y}(k)^2]}, \quad (16)$$

$$C_{\mathrm{P}} = \sqrt{\frac{1}{N}\sum_{k=0}^{N-1}\left[P(k)^2 - \bar{P}(k)^2\right]}. \quad (17)$$

The value of r, as listed in Table 1, directly implies the presence or absence of a macrocell user over the channel of interest. On computing r, the first decision box in the fine detection stage checks whether r is equal to 0. If this is true, then the test statistic turns out to be $\mathcal{H}_0$. Zero correlation between the received signal and the local pilots implies that the received signal is not an LTE-OFDM modulated macrocell user signal; rather, it is a mere random noise signal that escaped through the coarse detection stage. On the other hand, if r is not equal to 0, then the channel of interest is suspected to have a co-channel macrocell user. Hence, the next decision box in the fine detection stage checks the degree of similarity between $Y(k)$ and $P(k)$. If r holds a positive value, then there exists a strong correlation between $Y(k)$ and $P(k)$. Thus, the test statistic is determined as $\mathcal{H}_1$, thereby conditioning the maximum transmit power of a secondary femtocell user based on (11).

Alternatively, if the condition $0 < r \le 1$ is false, then there prevails a negative correlation between $Y(k)$ and $P(k)$. Therefore, the similarity between the received signal and the local reference pilots is known to be minimal. This is due to frequency offset in the received signal, which in turn, means that the received signal fails to match that of the local reference pilots. To handle such a frequency offset scenario, we implement

Table 1. Possible correlation coefficient values and corresponding hypotheses.

Cases	Correlation type	Hypotheses
$r = 0$	Zero correlation between $Y(k)$ and $P(k)$	$\mathcal{H}_0$
$0 < r \le 1$	Positive correlation pilot tones of $Y(k)$ correlate with pilot tones of $P(k)$	$\mathcal{H}_1$
$-1 \le r < 0$	Negative correlation pilot tones of $Y(k)$ do not correlate with pilot tones of $P(k)$	Frequency offset

a sliding frequency window (SFW) process. Let β be the portion of band in guard space G, over which the frequency offset is expected. The expected frequency offset β over guard space G is written as

$$\beta \in \left[-\frac{G}{2}, \frac{G}{2}\right]. \quad (18)$$

The SFW slides over the received signal with a frequency shift of β Hz and is expressed as

$$Y(k) \overset{\mathrm{SFW}}{\Rightarrow} Y(k+\beta). \quad (19)$$

For every β-shift in the received signal frequency, a new correlation value, $C_K(\beta)$, is calculated as follows:

$$C_K(\beta) = \sum_{k=1}^{N-1} \left|P(k)\right|^2 \times |\, Y(k+\beta)\,|^2 . \quad (20)$$

The collective correlation value $C_K(\beta)$ for different frequency shifts (β) is considered, and the maximum correlation result among all β frequency shifts is observed as $C_{\max}(\beta)$.

$$C_{\max}(\beta) = \arg\max_{\beta} C_K(\beta), \quad (21)$$

where $C_{\max}(\beta)$ determines the presence of a macrocell user over the channel of interest and accordingly the maximum transmit power of the femtocell user is optimized. In contrast, if the correlation between $Y(k)$ and $P(k)$ is still weak after all possible β frequency shifts, then the sensed channel is considered to be contaminated by traces of high-frequency pilots on a neighboring channel. Our PSS algorithm decides this channel state as idle. We obtain the test metric by averaging all the correlation results, which yields

$$\gamma = \frac{\max\{C_K(\beta)\}}{\frac{1}{\beta - 1}\left\{\sum_{\beta=\pm G/2} C_K(\beta)\right\}}. \quad (22)$$

On substituting (20) in (22), we have

$$\gamma = \frac{\max\left\{C_K(\beta)\right\}}{\frac{1}{\beta - 1}\left\{\sum_{\beta=\pm G/2}\left(\sum_{k=1}^{N-1}\left|P(k)\right|^2 \times \left|Y(k+\beta)\right|^2\right)\right\}}. \quad (23)$$

We synthesize (23) based on [20], which yields

$$\gamma = \frac{\max\{C_K(\beta)\}}{\sum_{\beta=\pm G/2}\left[\sum_{L}\left|\frac{\sqrt{A}n(i-v)}{\sqrt{\beta-1}}\right|^2\right]}, \tag{24}$$

where L is the number of pilot tones and A is the amplitude of a pilot tone in the time domain; $n(i-v)$ is the average Gaussian noise, characterized by zero mean and variance σ_n^2/M, where M is the length of extended segmentation. Through the infinite divisibility property of Gamma distribution, the denominator of (24) can be represented as

$$\sum_{\beta=\pm G/2}\left[\sum_{L}\left|\frac{\sqrt{A}n(i-v)}{\sqrt{\beta-1}}\right|^2\right] \approx \text{Gamma}\left((\beta-1)L, \frac{A\sigma_n^2}{M(\beta-1)}\right). \tag{25}$$

For greater values of β, the Gamma distribution yields very small values. Thus, by a mean approximation of the Gamma distribution, we have

$$\sum_{\beta=\pm G/2}\left[\sum_{L}\left|\frac{\sqrt{A}n(i-v)}{\sqrt{\beta-1}}\right|^2\right] \approx \frac{AL\sigma_n^2}{M}. \tag{26}$$

On substituting (26) in (24), the decision metric γ can be formulated as

$$\gamma = \frac{\max\{C_K(\beta)\}}{\frac{AL\sigma_n^2}{M}}, \tag{27}$$

$$\gamma = \max\left\{\sum_{L}\left|\frac{\sqrt{M}n(i-v)}{\sqrt{L\sigma_n^2}}\right|^2\right\}. \tag{28}$$

The decision is made by comparing the test metric γ with a preset correlation threshold value λ [20].

$$\lambda = \text{Gamma}^{-1}\left((1-P_{\text{f}})^{\frac{1}{\beta}}; L, \frac{1}{L}\right), \tag{29}$$

where P_{f} is the probability of deciding the channel hypothesis as $\mathcal{H}_0$ when the test metric γ is truly greater than the correlation threshold λ. That is,

$$P_{\text{f}} = P(\gamma > \lambda | \mathcal{H}_0), \tag{30}$$

$$P_{\text{f}} = 1 - \underbrace{\left[P\left(\sum_{L}\left|\frac{\sqrt{M}n(i-v)}{\sqrt{L\sigma_n^2}}\right|^2\right) \le \lambda \mid \mathcal{H}_0\right]^{\beta}}_{P_{\text{d}}},$$
$$P_{\text{f}} = 1 - \left[\text{Gamma}\left(\lambda; L, \frac{1}{L}\right)\right]^{\beta}. \tag{31}$$

Similarly, the probability of synchronization error (P_{se}) is the probability that a synchronization fails due to the occurrence of a false alarm at any instant prior to a frequency shift of β. This can be represented as

$$P_{\text{se}} = 1 - \left(\prod_{\beta=\pm G/2}\left(1 - P_{\text{f}}(\beta)\right)\right). \tag{32}$$

The smaller the synchronization error probability, the greater the chance of detecting the correct channel state. Therefore, a precise sensing duration (τ_{T}), a well-defined sensing band space ($B + G$), extended segmentation, SFW (β), instantaneous two-stage decisions, and desirable power optimization all help serve the PSS algorithm to avoid co-channel interference between a macro–femtocell heterogeneous network. With the aid of our PSS algorithm, some of the common spectrum sensing limitations, such as the detection of an unsynchronized macrocell user's signal as a noise signal and the high frequency traces of neighboring channel components as the presence of a macrocell user's information, are alleviated.

IV. Performance Analysis

In this section, we study the performance of our PSS algorithm through Matlab simulations. The PSS algorithm undergoes 1,000 Monte Carlo simulations. Table 2 lists the simulation parameters. A Rayleigh channel with a generalized Doppler spread of 222.22 Hz is considered.

Figure 5 shows the detection probabilities of the PSS algorithm, traditional energy detector and cyclostationary detector over different sensing durations. For a sensing duration of 5 μs, the detection probability of the PSS algorithm is 0.97,

Table 2. Simulation parameters.

Parameters	Values
Carrier frequency	2.5 GHz
System bandwidth	10 MHz
Modulation scheme	16-QAM
Number of bits/symbol	4
Symbol period	0.4 μs
Sensing duration	5.6 μs
Number of femtocells per macrocell	100
Number of active users per femtocell	4
Number of users per macrocell	2,000
Macrocell maximum transmit power	46 dBm
Femtocell maximum transmit power	15 dBm

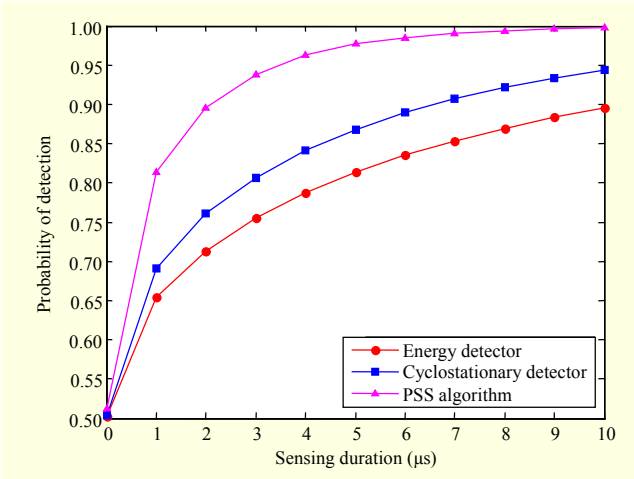

Fig. 5. Performance comparison between proposed and conventional spectrum sensing techniques at various sensing durations, at 4 dB SNR.

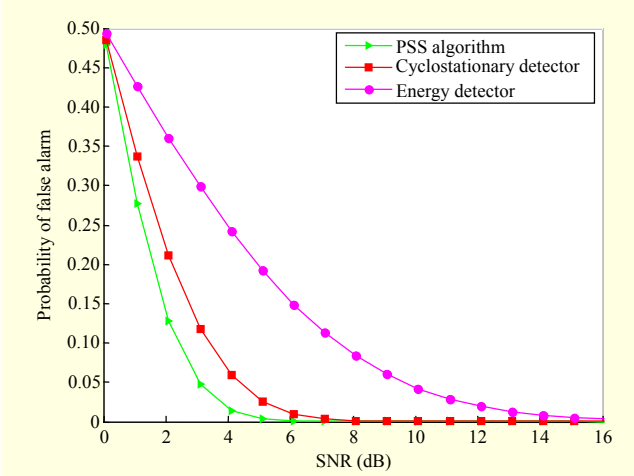

Fig. 6. Performance comparison between proposed and conventional spectrum sensing techniques for different SNR values.

whereas for cyclostationary and energy detection, the detection probabilities are 0.86 and 0.80, respectively. The performance improvement of our PSS algorithm is due to the validation of weak and uncertain macrocell user signals through the fine detection stage. On the other hand, cyclostationary and energy detection fails to identify weak macrocell user signals in the presence of dominant noise signals. Hence, on average, the PSS algorithm detects the presence of a macrocell user 11% better than that of the cyclostationary detection method and 17% better than that of the energy detection method.

Figure 6 illustrates the probability of false alarm for various SNR values. For a received SNR of 4 dB, the PSS algorithm yields a supportable false alarm probability of 0.02, whereas energy detection and cyclostationary detection methods yield

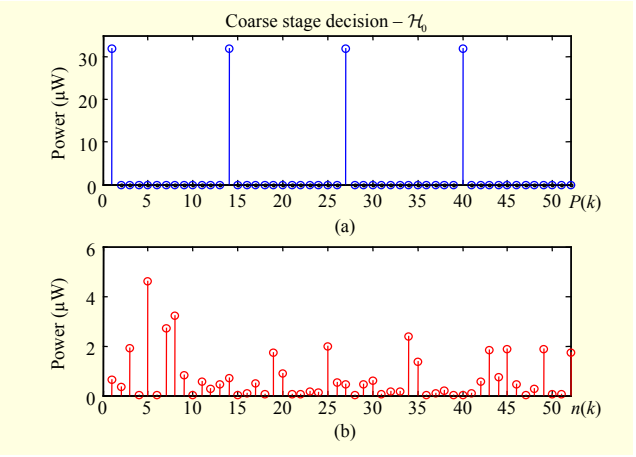

Fig. 7. Illustration of initial test statistic of coarse detection stage: (a) power of $P(k)$ in μW and (b) power of $n(k)$ in μW.

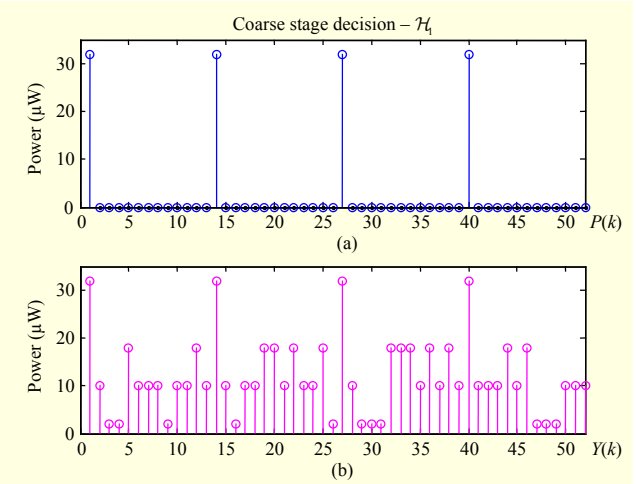

Fig. 8. Illustration of $\mathcal{H}_1$ test statistic in coarse detection stage of our PSS algorithm: (a) power of $P(k)$ and (b) power of $Y(k)$.

comparatively higher false alarm probabilities of 0.25 and 0.07, respectively. As cyclostationary and energy detection methods are highly sensitive to noise and do not focus on signals with time and frequency offsets, channels containing macrocell users can invariantly be miss-detected as idle. Hence, cyclostationary and energy detection methods have higher false alarm probabilities than the PSS algorithm.

Figure 7 illustrates the first test statistic of the coarse detection stage, where the power of local pilot tones is compared with the sensed signal power. For a sensing period of 20 μs, Fig. 7(a) shows that the power of local pilot tones is 32 μW. On the other hand, Fig. 7(b) indicates that the power of the sensed signal is just 5 μW — one-sixth that of the local pilot tones. The weaker power of the sensed signal implies the absence of dominant power pilots in the received signal. Hence, the channel of interest is decided as idle ($\mathcal{H}_0$).

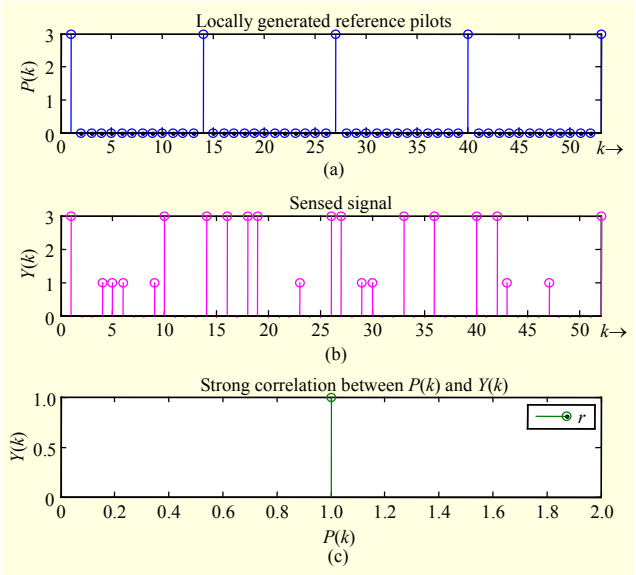

Fig. 9. Strong correlation between $Y(k)$ and $P(k)$: (a) local pilot tones $P(k)$, (b) sensed macrocell user's signal $Y(k)$, and (c) correlation coefficient (r) reaches 1 at maximum values of $Y(k)$ and $P(k)$.

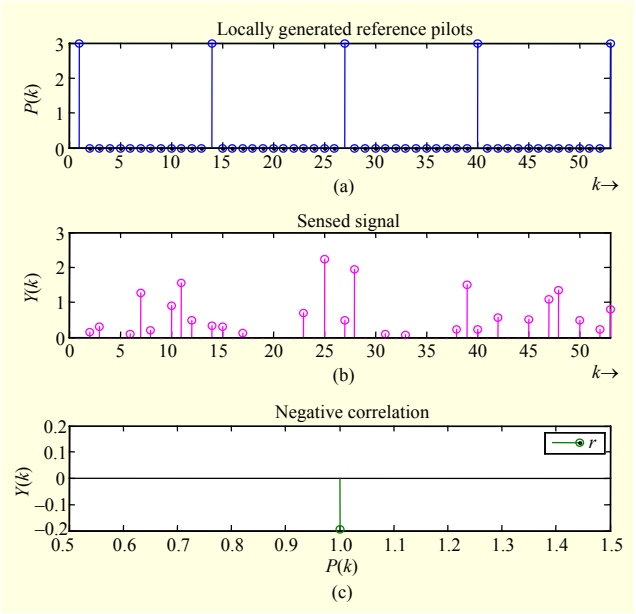

Fig. 10. Weak correlation between $Y(k)$ and $P(k)$: (a) local pilot tones $P(k)$, (b) sensed signal $Y(k)$ with channel impairments, and (c) correlation coefficient (r) holds negative value.

The second test statistic of the coarse detection stage is shown in Figs. 8(a) and 8(b). It is inferred that the power of the local pilot tones exactly matches with that of pilots in the sensed signal. A dominant sensed pilot-power guarantees the presence of a co-channel macrocell user, thereby ensuring the channel state as busy. The three levels of correlation in the fine detection stage are illustrated in Figs. 9, 10, and 11, respectively.

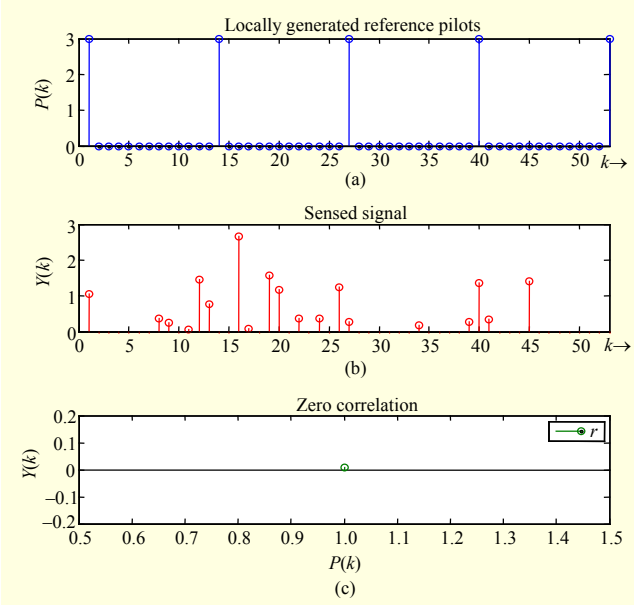

Fig. 11. Zero correlation between $Y(k)$ and $P(k)$: (a) local pilot tones $P(k)$, (b) sensed noisy signal $Y(k)$, and (c) correlation coefficient tends to be zero.

Figures 9(a), 9(b), and 9(c) show the local reference pilots, the sensed signal, and the degree of correlation between them. As pilots in the received signal exactly match with local reference pilots, the sensed channel of interest is decided as busy. The maximum correlation between $P(k)$ and $Y(k)$ infers that the sensed signal is free from time and frequency offsets, which indeed is not practical to consider. To deal with time and frequency offsets, our PSS algorithm is incorporated with extended segmentation and SFW.

Figure 10(c) exemplifies a negative correlation between the received signal and the local pilots. The SFW of the PSS algorithm handles frequency offset by sliding the sensed signal frequency by a band space of β. For every β shift, the sensed signal is correlated with local pilots to reach maximum correlation. On attaining maximum correlation, the channel of interest is decided as busy.

Figure 11(c) illustrates a zero correlation between $P(k)$ and $Y(k)$. It should be noted that the sensed signal is a mere random noise signal; hence, the fine detection stage decides the channel state as idle.

The fairer the sensing time (ST), the higher the chance of detecting the correct channel status. Figure 12 depicts that the PSS algorithm attains an effective detection probability of 0.90 with an appreciable sensing period of 4 μs and SNR of 6 dB. For a sensing period of 8 μs, the probability of detection reaches 1 with the same SNR of 6 dB. Hence, our PSS algorithm increases the detection probability with increasing sensing duration. It is also observed that the SNR required by the PSS algorithm to attain a maximum detection probability is

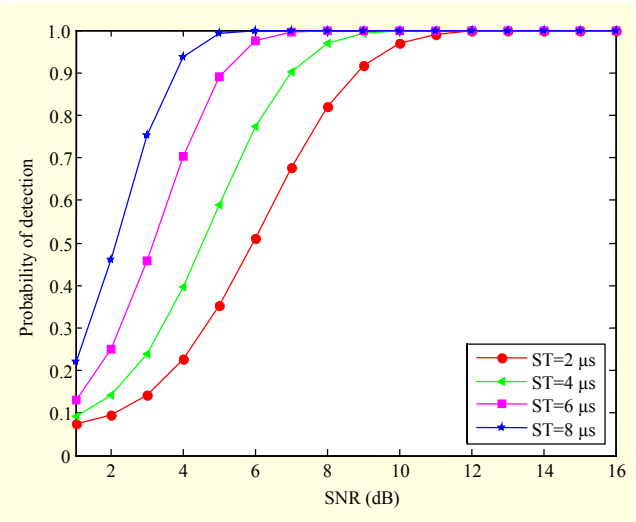

Fig. 12. Probability of detection vs. SNR for various sensing periods in PSS algorithm.

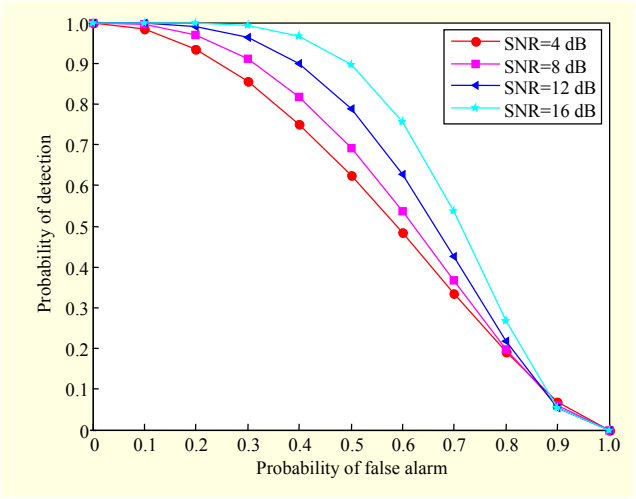

Fig. 13. ROC for PSS at different SNR values ($\tau_T = 6$ μs).

reduced by 2 dB for every 2 μs increase in sensing duration. The receiver operating curve (ROC) shown in Fig. 13 illustrates the performance of our PSS algorithm at different SNR values with a fixed sensing duration of 6 μs.

For the comfortable SNR of 16 dB and with a false alarm probability of 0.3, the probability of detection remains at 1. On the other hand, at a lower SNR of 5 dB and with a false alarm probability of 0.4, the PSS algorithm attains a detection probability of 0.75. The above simulation results show that the PSS algorithm attains an appreciable detection probability and minimum false alarm probability at poor received SNR but acceptable sensing duration. Hence, the PSS algorithm is highly sensitive in detecting the presence of a macrocell user with poor signal quality. This attribute of the PSS algorithm helps in avoiding co-channel interference.

Generally, the false alarm probability of a sensing system will be higher at a weaker received SNR as well as insufficient sensing duration. Nevertheless, our simulation results indicate that the PSS algorithm still manages to attain a tolerable false alarm probability with significantly less sensing duration, thereby contributing to a robust sensing system.

V. Conclusion

In this paper, we proposed a pilot-based spectrum sensing (PSS) algorithm to handle co-channel interference between macro–femtocell networks. The PSS algorithm efficiently tests the existence of a co-channel macrocell user over the channel of interest. Upon detecting the presence of a co-channel macrocell user, the proposed system instantaneously conditions the maximum transmit power of the interfering femtocell user. Precise sensing bandwidth, limited sensing duration, extended segmentation, and sliding frequency window equip the PSS algorithm to be more robust against time and frequency offsets. Performance analysis exemplifies that even at low received SNRs and sensing durations, the PSS algorithm obtains higher detection and lower false alarm probabilities, whereas this cannot be said of conventional sensing techniques.

References

[1] M. Reardon, *Cisco Predicts Wireless-Data Explosion*, Cisco Press Release, Feb. 9, 2010. Accessed June 2013. http://www.cnet.com/news/cisco-predicts-wireless-data-explosion/

[2] U. Jang et al., "Interference Management with Block Diagonalization for Macro/Femto Coexisting Networks," *ETRI J.*, vol. 34, no. 3, June 2012, pp. 297–307.

[3] T. Yucek and H. Arslan, "A Survey of Spectrum Sensing Algorithm for Cognitive Radio Application," *IEEE Commun. Surveys Tutorials*, vol. 11, no. 1, 2009, pp. 116–130.

[4] L. Gavrilovska et al., "Learning and Reasoning in Cognitive Radio Networks," *IEEE Commun. Surveys Tutorials*, vol. 15, no. 4, 2013, pp. 1761–1777.

[5] B. Shen and K.S. Kwak, "Soft Combination Schemes for Cooperative Spectrum Sensing in Cognitive Radio Networks," *ETRI J.*, vol. 31, no. 3, June 2009, pp. 263–270.

[6] A. Mariani, A. Giorgetti, and M. Chaini, "Effect of Noise Power Estimation on Energy Detection for Cognitive Radio Applications," *IEEE Trans. Commun.*, vol. 59, no. 12, Dec. 2011, pp. 3410–3420.

[7] K.W. Choy, W.S. Jeon, and D.G. Jeong, "Sequential Detection of Cyclostationary Signal for Cognitive Radio System," *IEEE Trans. Wireless Commun.*, vol. 8, no. 9, Sept. 2009, pp. 4480–4485.

[8] S.S. Hwang, D.C. Park, and S.C. Kim, "Frequency Domain DTV Pilot Detection Based on the Bussgang Theorem for Cognitive Radio," *ETRI J.*, vol. 35, no. 4, Aug. 2013, pp. 644–654.

[9] A. Bagwari and G.S. Tomar, "Multiple Energy Detection and Cyclostationary Feature Detection Spectrum Sensing Technique," *Int. Conf. Commun. Syst. Netw. Technol.*, Bhopal, India, Apr. 7–9, 2014, pp. 178–181.

[10] J. Lundén et al., "Collaborative Cyclostationary Spectrum Sensing for Cognitive Radio Systems," *IEEE Trans. Signal Process.*, vol. 57, no. 11, Nov. 2009, pp. 4182–4195.

[11] A. Bagwari, G.S. Tomar, and S. Verma, "Cooperative Spectrum Sensing Based on Two-Stage Detectors with Multiple Energy Detectors and Adaptive Double Threshold in Cognitive Radio Networks," *Canadian J. Elect. Comput. Eng.*, vol. 36, no. 4, 2013, pp. 172–180.

[12] Y. Li and S.K. Jayaweera, "Dynamic Spectrum Tracking Using Energy and Cyclostationarity-Based Multi-variate Non-parametric Quickest Detection for Cognitive Radios," *IEEE Trans. Wireless Commun.*, vol. 12, no. 7, July 2013, pp. 3522–3532.

[13] Z. Lu et al., "Novel Pilot-Assisted Spectrum Sensing for OFDM Systems by Exploiting Statistical Difference between Subcarriers," *IEEE Trans. Commun.*, vol. 61, no. 4, Apr. 2013, pp. 1264–1276.

[14] Q. Li et al., "Joint Access and Power Control in Cognitive Femtocell Networks," *Int. Conf. Wireless Commun. Signal Process.*, Nanjing, China, Nov. 9–11, 2011, pp. 1–5.

[15] W. Wang, G. Yu, and A. Huang, "Cognitive Radio Enhanced Interference Coordination for Femtocell Network," *IEEE Commun. Mag.*, vol. 51, no. 6, June 2013, pp. 37–43.

[16] S.-M. Cheng et al., "On Exploiting Cognitive Radio to Mitigate Interference in Macro/Femto Heterogeneous Networks," *IEEE Wireless Commun.*, vol. 18, no. 3, June 2011, pp. 40–47.

[17] D. Min, L. Tong, and B.M. Sadler, "Optimal Insertion of Pilot Symbols for Transmissions over Time-Varying Flat Fading Channels," *IEEE Trans. Signal Process.*, vol. 52, no. 5, May 2004, pp. 1403–1418.

[18] 3GPP LTE Release 11, *Tech. Specification of 3GPP LTE Radio Specification,* Sept. 2013.

[19] T.-D. Chiueh and P.-Y. Tsai, "*OFDM Baseband Receiver Design for Wireless Communication*," Taipei, Taiwan, John Wiley & Sons Pte. Ltd, 2008, pp. 115–118.

[20] H. Li, X. Wang, and J. Nadeau, "Robust Spectrum Sensing for OFDM Signal without Synchronization and Prior Noise Knowledge," *Wireless Commun. Mobile Comput.*, vol. 14, no. 6, Apr. 2014, pp. 644–658.

Padmapriya Sambanthan received her BTech and MTech degrees in electronics and communication engineering from Pondicherry University, Puducherry, India, in 2010 and 2012, respectively. She is currently pursuing a full-time PhD course at Pondicherry Engineering College, Puducherry, India, under a TEQIP grant. Her research interests include macro–femtocell heterogeneous networks, interference avoidance techniques, and radio resource management in 3GPP LTE systems.

Tamilarasi Muthu received her ME degree in electronics engineering from the Madras Institute of Technology, Chennai, India, in 1991 and her PhD degree in electronics and communication engineering from Pondicherry University, Puducherry, India, in 2009. She currently holds an academic post as professor in the Department of Electronics and Communication Engineering, Pondicherry Engineering College, Puducherry, India. Her research interests include MIMO, multiuser communications, interference rejection, iterative receiver algorithms, and error-correction coding.